Convection in vertical annular gap formed by stationary heated inner cylinder and rotating unheated outer cylinder

V. K. Chithrakumar, G. Venugopal & M. R. Rajkumar

Heat and Mass Transfer
Wärme- und Stoffübertragung

ISSN 0947-7411

Heat Mass Transfer
DOI 10.1007/s00231-019-02614-0

Springer

Heat and Mass Transfer
https://doi.org/10.1007/s00231-019-02614-0

ORIGINAL

Convection in vertical annular gap formed by stationary heated inner cylinder and rotating unheated outer cylinder

V. K. Chithrakumar[1] · G. Venugopal[2] · M. R. Rajkumar[1]

Received: 30 July 2018 / Accepted: 22 March 2019

Abstract

A combined experimental and numerical study was conducted to understand the effect of rotation of outer cylinder on heat transfer from a vertical heated inner cylinder. The dimensionless analysis carried out for this problem underlines that the non dimensional heat transfer depends on the rotation parameter, radius ratio and aspect ratio. Experiments were conducted for the rotational parameter ranging from $0 \leq \zeta \leq 526$ at different heat loads, keeping the aspect ratio and radius ratio unchanged. Numerical simulations have been performed (for a wide range of rotation parameter $0 \leq \zeta \leq 526$ and fixed radius ratio) using a commercial computational fluid dynamics package ANSYS CFX 14. The heat transfer was found to increase progressively with increasing rotational parameter until a certain value of rotational parameter was reached, thereafter a sharp decay in heat transfer resulting from destabilization of flow field was observed. Three laminar heat convection modes, namely; natural, mixed and forced convection dominant, have been observed during the increasing phase of Nusselt number with rotation parameter. The transport mechanism under different heat transfer regimes was explored and discussed with the aid of numerically simulated flow and thermal fields.

Keywords Convection · Vertical annulus · Rotation parameter · Centrifugal force · Buoyant force

Nomenclature

A	Surface area of heated stationary inner cylinder, m^2
d	Annular gap, D_o-D_i, m
g	Acceleration due to gravity, m/s^2
H	Height of the annulus, m
h	Convective heat transfer coefficient, W/m^2K
k	Thermal conductivity, W/mK
p	Pressure, Pa
Q	Heat input, W
q''	Heat flux, W/m^2
r	Radial distance, m
T	Temperature, K
V	Velocity vector, m/s
Gr	Grashof number, $\frac{g\beta\Delta T d^3}{\nu^2}$
Greek symbols	
η	Radius ratio, $\frac{r_i}{r_o}$
ζ	Rotation parameter, $\frac{Re_\omega^2}{Gr}$
ω	Angular velocity, rad/s
ρ	Density, kg/m^3
α	Thermal diffusivity, m^2/s
β	Isobaric cubic expansivity of fluid, 1/K
ν	Kinematic viscosity, m^2/s
σ	Standard deviation
Subscripts	
avg	Average
atm	Atmospheric
b	Bulk
f	Fluid
i	Inner
o	Outer
0	Stagnation
∞	Free stream

Highlights
- Experimental, numerical studies of heat transfer in vertical annular gap
- Annular gap between heated stationary inner cylinder and outer rotating cylinder
- Heat transfer from heated inner cylinder increased with outer cylinder speed
- After a critical value of outer cylinder speed heat transfer decreases
- The physics of flow and energy transport mechanism was explored and discussed

✉ M. R. Rajkumar
rajkumar@cet.ac.in

Extended author information available on the last page of the article.

Published online: 07 May 2019

1 Introduction

Convection in stationary cylindrical annulus had been a subject of fundamental interest to many earlier researchers [1–7] because of the complex nature of flow and thermal fields that characterizes the thermal transport phenomena. The complexity adds when rotation is given to one or both walls of the cylindrical annulus. This is due to the fact that flow and thermal fields are greatly influenced by the swirl component of velocity induced by the active centrifugal force, in addition to the axial and radial component of velocity. The development of new rotating devices of technological importance such as rotating electrical machines, rotating heat exchangers, clinical blood oxygenators, gas centrifuges and many others have prompted further simulated interest in this area. Consequently, considerable research efforts in understanding convection in rotating annulus have been reported in the literature. Fujio et al. [8] studied experimentally convection in the annular gap between horizontal rotating inner cylinder and stationary outer cylinder at different rotational speeds and annular spaces. They reported that at narrow annular space and low rotational speeds, the flow is laminar and the heat transfer is mainly by conduction and radiation. However, as the rotational speed increases the heat transfer was found to increase as a result of secondary vortices induced by the centrifugal forces. Kuzay et al. [9] conducted experimental investigations to study forced convection in a large-gap vertical annulus with stationary as well as rotating inner cylinder. Their study revealed that the temperature field in the annular gap was influenced by the rotation of the inner cylinder. A correlation was established between rotational and non rotational Nusselt number as a function of hydraulic diameter, diameter of inner cylinder and rotation ratio. A finite-difference scheme was proposed by Sarhan et al. [10] for solving the boundary layer equations of laminar free convection flow in open ended vertical concentric annuli of radius ratio 0.5 with rotating inner wall. It was reported by the authors that for high values of dimensionless volumetric flow rate, rotational effect causes fluid to move from regions close to the two boundaries to the core. But for low values of volumetric flow rate the fluid from the region close to the adiabatic wall was observed to displace to the region close to the heated wall. Numerical results were presented by El-Shaarawi et al. [11] for the combined free and forced convection developing laminar boundary layer flow in a vertical concentric annulus with a rotating inner cylinder. In this study they analyzed the effect of rotating inner cylinder on the hydrodynamic developing length, critical distance at which axial velocity gradient normal to the wall vanishes and the heat transfer performance. Toru et al. [12], conducted numerical analysis for two-dimensional mixed convection in horizontal concentric annlus with a heated rotating inner cylinder for a fixed ratio of the annulus gap width to the inner cylinder radius. The study successfully demonstrated the applicability of the vorticity-velocity formulation in solving fluid flow and heat transfer problems within the domain wherein mass flow rates are not known a priori. Hessami et al. [13] studied, numerically laminar convection in an air contained enclosure formed between two vertical, concentric cylinders and two horizontal planes. The rotating inner cylinder and one of the horizontal planes were heated were as the other horizontal plane and outer cylinder were maintained at low temperatures. Their study concluded that at low values of radius ratio and high values of rotational Reynolds number the centrifugal effect becomes the dominant factor influencing the flow and thermal field, whereas, at high aspect ratios and low Rayleigh numbers the dominance of buoyancy effects was evident. Ball and Farouk [14] conducted a numerical study to determine the heat transfer characteristics and flow patterns around a heated and rotating vertical cylinder enclosed in a stationary outer cylinder with fixed, adiabatic horizontal end-plates. The effect of buoyancy forces by heating the inner cylinder, on the development of the Taylor vortex flow was examined and reported that first, the formation of the Taylor vortices was suppressed by the buoyancy for values of the rotational parameter $\sigma = \mathrm{Gr}/\mathrm{Re}^2$ greater than unity. Below $\sigma = 1.0$, Taylor vortices first appear, with the cells developing at the top of the annulus. In the mixed-convection region ($0.01 < \sigma < 1.0$), a distorted form of the Taylor cells is observed, with the cell rotating in the same sense. As σ was decreased below $\sigma = 0.01$, the isothermal flow patterns were eventually recovered. Ball et al. [15] conducted experiments to study interdependence between the heat transfer mechanism and structure of secondary flows in an annular gap between concentric vertical cylinders. The heated and rotating inner cylinder was aligned concentrically with stationary and cooled outer cylinder. They elucidated the qualitative aspect of mixed convection flows in vertical annular enclosures in terms of the value of Froude number. They found that physical existence of secondary flows was significantly affected by buoyancy till the Froude number reaches the critical value 0.01. At values of Froude number lower than 0.01 the cell pattern remains unchanged even though the strength of the secondary flow increases. Stability of axial flow between concentric cylinders with the inner cylinder rotating was experimentally investigated by Lueptow et al. [16]. With an imposed axial pressure gradient seven flow regimes of toroidal vortices, including Taylor vortices, wavy vortices, random wavy vortices, modulated wavy vortices, turbulent modulated wavy vortices, turbulent wavy vortices, and turbulent vortices were identified. Rothe et al. [17] investigated both experimentally and numerically, turbulent flow and heat transfer in a concentric annulus between two rotating cylinder tubes. Numerical computations were done for the case of heated outer cylinder and

adiabatic inner cylinder, and also by reversing the heat conditions on the cylindrical walls. They have reported the efficacy of Reynolds stress turbulence model and mixing length turbulence model for the first and second cases respectively, and shown that the numerical and experimental results compare well. Turbulent mixed convection of air in a concentric horizontal annulus between cooled outer cylinder and a heated rotating inner cylinder was numerically investigated by Char and Hsu [18]. Simulations were conducted for Rayleigh number, ranging from 10^7 to 10^{10}, the Reynolds number, from 0 to 10^5 and the radius ratio, from 2.6 to 10 for a constant Prandtl number of 0.7. The authors reported that for all the configurations the mean Nusselt number increases with increase in Rayleigh number, decreases with increase in Reynolds number and radius ratio. One of the important findings of this study was that for $Ra > 10^9$, corresponding to strong buoyancy driven turbulent flow the peak value of the Nusselt number distribution occurs in the visibility of thermal plume region. Mixed convection of air with $Pr = 0.7$ between two horizontal concentric cylinders maintained at different uniform temperatures was numerically investigated by Yoo and Sik [19]. It was reported that for small Rayleigh numbers with increase in rotational speed of the outer cylinder the point of maximum and minimum heat fluxes at the inner and outer cylinders move in the same direction of rotation, but for high Rayleigh numbers with increase in speed of the outer cylinder the point of maximum and minimum local heat fluxes at the inner and outer cylinders move in the same direction of rotation, but for high Rayleigh numbers no such trend was observed. A numerical study conducted by Lee [20] considered mixed recirculatory fluid motion and heat transfer in the annular space between two horizontal cylinders when the inner cylinder is heated and rotated. The Reynolds number range was so chosen that the effect of centrifugal acceleration and three dimensional Taylor vortices were considered to be negligible. When the inner cylinder was made to rotate, a Couette like flow in the form of concentric circles that surrounds the inner cylinder was observed. As rotational speed increases the thermal plume tilts in the direction of rotation with a reduced amplitude and eventually resulted in a single thermal plume moving in the direction opposite to the direction of rotation of inner cylinder. Steady laminar mixed convection in the fully developed region of horizontal concentric annuli was investigated numerically by Habib and Negm [21] for the case of non-uniform circumferential heating. Two cases of non uniform heating were studied viz 1 uniform heating of top half of inner cylinder while the bottom half is kept insulated and 2 heated and insulated surface were reversed. They reported that the the configuration with heating on the top half showed better heat transfer performance than with bottom heating configuration due to presence of weak secondary flow caused by temperature stratification. A numerical investigation to study the effect of rotation on the axisymmetric flow driven by buoyancy in an annular cavity was reported by Venkatachalappa et al. [22]. The inner and outer sidewalls are maintained at constant temperature while the top and bottom walls are adiabatic. The computational results reveal that the rate of heat transfer at the hot cylinder is suppressed when its speed of rotation is higher than that of the cold cylinder. Lee et al. [23] conducted numerical simulations for upward air flow in a vertical pipe with rotating outer wall. Their study revealed that the rotation of outer wall greatly influences the turbulent structures causing suppression of turbulent motion near the rotating wall and enhancement of the turbulent intensity close to the stationary wall. Also they have noticed that with increase in rotational speed the turbulence at the stationary wall was found to increase which in turn resulted in the hike of turbulent velocity near the stationary wall. The study on air gap convection in rotating electrical machines by Howey et al. [24] reported that the air-gap convective heat transfer is affected primarily by the rotating speed of the machine, size of the rotor and air gap.

The literature study pertinent to convective heat transfer in rotating concentric cylindrical annulus unveils that most of the works so far have been performed to understand transport of thermal energy in rotating horizontal cylindrical annulus and, comparatively, fewer studies were reported to address convection in rotating vertical cylindrical annulus. Also, in most of the above cases the inner cylinder was rotating and the outer cylinder was kept stationary. Furthermore, the problems were studied numerically. In the present work the focus is to study both experimentally and numerically, convection in a vertical annulus wherein heated inner cylinder is stationary and cold outer cylinder is rotating. Here the principle attention is to study the influence of induced flow originated by the rotational effect of the outer cylinder on the natural convection plume emanating from the stationary heated vertical cylinder and also to simulate numerically the hydrodynamic and thermal field for a better understanding of the thermal transport phenomena.

2 Experimental setup

Schematic of the experimental facility is given in Fig. 1. The experimental facility consists of annular space formed by two concentric vertical cylinders. The inner cylinder is a polished hollow copper tube of outer diameter 51 mm, thickness 3 mm and height 620 mm. The outer cylinder is made of acrylic tube of inner diameter 83 mm, thickness 5 mm and height 620 mm. The aforesaid dimensions of the cylinders forms an annular gap having a radius ratio of $\eta =$

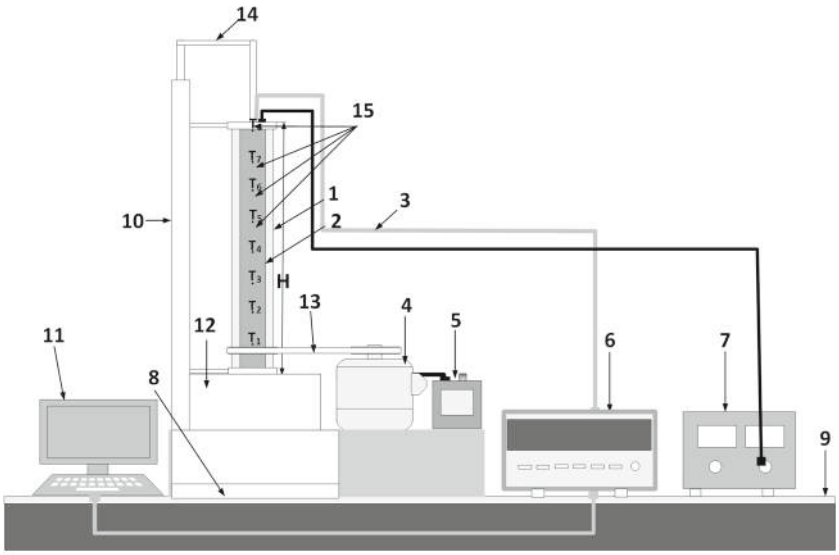

Fig. 1 Schematic of experimental setup

1. Rotating Outer Cylinder, 2. Heated Inner Cylinder, 3. Thermocouple wires, 4. Three Phase AC motor, 5. Variable Frequency drive, 6. Data Acquisition System, 7. DC Power Supply, 8. Opening, 9. Optical Bench, 10. Frame, 11. Computer 12. Plenum, 13. Belt drive, 14. Adjustable clamp holding the heater, 15. Thermocouple positions

0.614 that comes under the limit of moderate gap annulus [25]. The inner copper tube is heated with a cartridge heater, that has been inserted from the top of the copper tube. The cartridge heater is having a ceramic bush at its top that act as an insulator to heat transmission from the end face of the copper tube. It is worth to note that the outer dimension of the ceramic bush is same as the outer diameter of the copper tube. The cartridge heater, ceramic bush and copper tube form as an integral body which is clamped to a frame with provisions for adjusting the vertical alignment of the inner cylinder (see Fig. 1). At the bottom end of the copper tube, a Teflon rod of diameter same as the outer diameter of the copper tube is inserted to prevent the heat loss from bottom end face of the copper tube. Further, the Teflon rod, is fixed to the frame of the assembly, thereby, enacting as a support for the bottom end of the copper tube. The inner copper tube is aligned vertically, before fixing the outer tube, and the vertical alignment of the inner tube is ensured using a spirit level. The cartridge heater is heated at various heat loads by applying regulated DC power (Aplab India Ltd).

The outer cylinder is mounted concentrically by two nylon bearings, one at the top and the other at the bottom. These bearings are supported by brackets which in turn are fixed to the frame of the assembly. The nylon bearings facilitates smooth rotation of the outer cylinder and at the same time they arrest the axial movement of the outer cylinder that may happen due to rotation. The outer cylinder carries a nylon pulley which is driven by a pulley connected to three phase AC motor (ABB India Ltd), through an open belt drive. The speed of rotation of the motor is controlled by Variable Frequency Drive, (Fuji, Electric, Japan). Care is taken to arrange the driver and driven pulleys close to each other such that the central distance between the pulleys is 150 mm. The speed of rotation of the outer cylinder is measured using a stroboscope (Mextech Technologies India Pvt Ltd). A dial gauge is used to check the eccentricity of outer cylinder during rotation and the eccentricity was found to be within $\pm$ 5 microns. A plenum is arranged at the bottom of the concentric annulus to avoid disturbances from the surroundings.

A total of sixteen T type calibrated thermocouples (32 SWG), eight thermocouples diametrically opposite to each other are fixed to the heated inner cylinder to measure the temperature at different locations of the cylinder. Longitudinal grooves where machined along the axial direction at different locations on the inner surface of the copper tube for embedding the thermocouple wires. The thermocouple wires were taken out from the top end of the inner cylinder. The thermocouples are located equidistantly from bottom to top of the inner cylinder. All the thermocouples are fixed to the respective positions by using highly conducting cement thermobond (Fabricka India Ltd.). Four stainless steel sheathed thermocouples arranged on a ring at the exit section of the annulus are used to measure the bulk outlet fluid temperature. Another two T type thermocouples are used in the plenum to measure the the temperature of the fluid at the inlet of the annulus. The calibration error of the thermocouples is estimated as 0.2 °C. The thermocouples are connected to a Personal computer based data acquisition system (Keysight India Ltd). The

entire assembly is mounted on an optical bench with the help of vibration isolators (rubber boots).

3 Data analysis and uncertainty estimation

3.1 Data analysis

The average temperature rise of inner heated cylinder is estimated by Eq. 1

$$\Delta T_{avg} = \frac{\sum_{j=1}^{N} T_j}{N} - T_f \tag{1}$$

Where $N = 16$

$$T_f = \frac{T_b + T_\infty}{2} \tag{2}$$

Where T_b is the bulk fluid temperature evaluated at the outlet, as per the procedure outlined in [26]

The rotational Reynolds number is calculated as:

$$\text{Rotational Reynolds number, } Re_\omega = \frac{\omega r_o d}{\nu} \tag{3}$$

The average heat transfer coefficient and average Nusselt number are defined respectively as:

$$h_{avg} = \frac{Q}{A\Delta T_{avg}} \tag{4}$$

$$\text{Nusselt number, } Nu_{avg} = \frac{h_{avg} d}{k_f} \tag{5}$$

3.2 Uncertainty estimation

The uncertainties in the estimated parameters is computed by the method suggested by Kline and McClintock [27] and [28]. The uncertainty in the independently measured data such as geometrical dimensions, surface temperature of the heated inner cylinder, fluid temperature, voltage, current and rotational speed of the outer cylinder is used to compute the uncertainty in estimated parameters: heat transfer rate (Q), average heat transfer coefficient (h_{avg}), average Nusselt number (Nu_{avg}), rotational Reynolds number (Re_ω) and rotation parameter (ζ), using Eq. 6. The procedure is detailed in Appendix. The uncertainties in the independently measured data is obtained either from the manufactures specification or calibration of instruments.The uncertainty in the values of the estimated parameters for a given heat flux $q'' = 80\ W/m^2$, and corresponding to high and low rotational speed, shown in Table 1 reveals that maximum uncertainty in the estimated parameter is less than 2.6%. The uncertainty in the estimated parameters for other heat loads are also calculated but not shown here for brevity.

$$\sigma_R = \sqrt{\pm\left\{\sum_{i=1}^{n}\left[\left(\frac{\partial R}{\partial X_i}\right)^2 \sigma_{X_i}^2\right]\right\}} \tag{6}$$

4 Numerical methodology

The mathematical model representing the momentum and energy transport in cylindrical coordinates along with the boundary conditions are:

4.1 Governing equations

a) Fluid domain

$$\nabla.\mathbf{V} = 0 \tag{7}$$

$$\frac{DV}{Dt} = -\frac{1}{\rho}\nabla P + \nu\nabla^2\mathbf{V} + \mathbf{S} \tag{8}$$

where $\mathbf{S}$ is the body force vector defined by

$$S = -g\beta(T - T_\infty)\hat{e_z} + -\frac{v^2}{r}\hat{e_r}$$

$$\frac{DT}{Dt} = \alpha\nabla^2 T \tag{9}$$

4.2 Boundary conditions

No slip for velocity components and zero normal pressure gradient are the boundary conditions given on all fluid-wall interfaces. Since the velocity components at the inlet and exit of the extended domain are not known as a priori for the density driven flow, they are obtained from the appropriate pressure boundary conditions imposed at the respective locations. With this in view, the stagnation pressure at the inlet of the extended domain is equated to the atmospheric pressure whereas static pressure at

Table 1 Uncertainty of the various measured and estimated parameters

		Measured						Estimated						
		$D_{i,o}$, d (mm)	H (mm)	T (°C)	V (V)	I (A)	N (rpm)	A (%)	Q (%)	h_{avg} (%)	Nu_{avg} (%)	Reω (%)	Gr (%)	ζ (%)
Q = 8W	N = 50 rpm	0.01	1.0	0.20	0.10	0.01	1.0	0.16	2.2	2.5	2.6	1.9	1.5	0.41
	N = 440 rpm	0.01	1.0	0.20	0.10	0.01	1.0	0.16	2.2	2.3	2.3	2.0	2.1	0.68

the exit of the extended domain is taken as atmospheric. Mathematically, the boundary conditions can be described as follows

$$V = 0, \quad \frac{\partial p}{\partial n} = 0, \quad at\ r = r_i \tag{10}$$

$$u = w = 0, \quad v = r_0\omega_o, \quad \frac{\partial p}{\partial n} = 0, \quad \frac{\partial T}{\partial n} = 0, \quad at\ r = r_0 \tag{11}$$

Pressure $p_0 = p_{atm}$, Temperature $T = T_\infty$ at the inlet of the extended domain and Pressure $p = p_{atm}$, $\frac{\partial T}{\partial y} = 0$ at the exit of the extended domain.

Aforementioned equations have been solved, numerically, using the commercial Computational Fluid Dynamics software ANSYS CFX 14 [29]. The physical domain and the corresponding computational domain employed for the numerical analysis are shown in Figs. 2, 3 respectively. The three dimensional computational domain was discretized using structured non-uniform hexahedral cells created by commercial meshing software Hypermesh 13 [30]. Fine grids with first layer thickness of 0.5 mm were employed in the proximity to both cylinder walls to resolve accurately velocity and temperature fields in the boundary layer.

4.3 Numerical solution procedure

The heated stationary inner cylinder is modeled as a cylindrical wall subjected to constant heat flux condition. The outer cylinder is adiabatic and is given rotation with a constant angular velocity ω. The top and bottom walls of the inner cylinder are thermally insulated. The fluid medium is air and is treated as in-compressible with constant thermophysical properties except density that varies only in the gravitational body force term in the vertical direction (z direction) and is modeled using Bousinesq approximation [31]. The validity of Boussnesq approximation for this kind of problem has been reported earlier in [32]. The viscous term in the energy equation is neglected.

The segregated steady state solver in CFX platform was chosen for the numerical computation. A second order upwind scheme is used to interpolate the unknown cell interface values required for modeling the convection terms. SIMPLE algorithm is used for pressure velocity coupling. The under relaxation factors used in the present study are 0.3 for pressure, 0.7 for momentum, 0.9 for energy. Convergence of the solution was set to be achieved when maximum of all the residues reaches less than 1×10^{-5}, to ensure conservation of quantities.

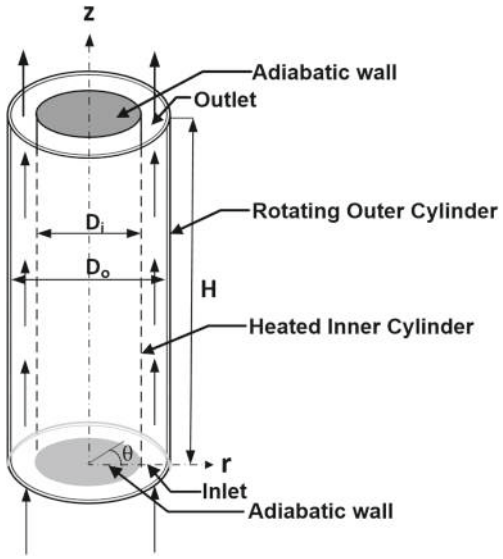

Fig. 2 Schematic of the physical configuration

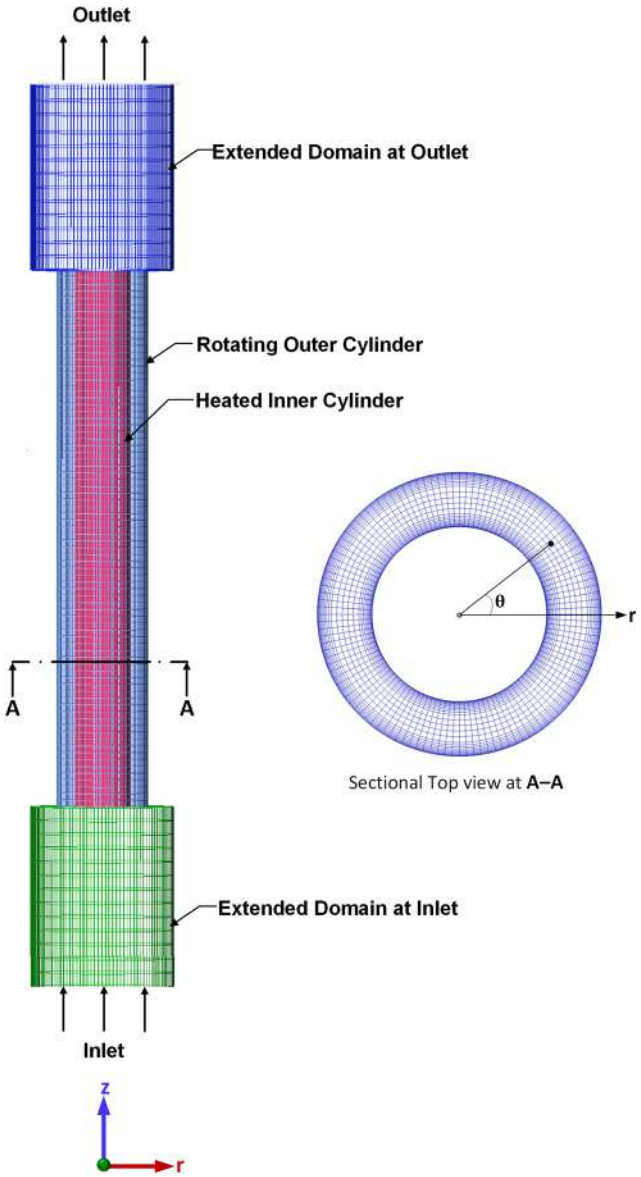

Fig. 3 Computational domain along with grid

As part of validation exercises, firstly, the problem was studied for the numerical solution of natural convection in vertical annulus considered in the experimental work. Initially, the numerical simulations were carried out in a computational domain without extended regions at the inlet and exit of the annulus. The comparison of numerically simulated local temperature and experimentally measured local temperature showed marked difference and the cause for the mismatch was reasoned due to the unknown velocity at the inlet of the computational domain, as reported by earlier researchers [33, 34] and [35]. This observation had become motivation for using extended domain at the inlet and exit sections of the annulus for the numerical computations. In accordance with this, simulations have been carried out by extending the domain at inlet and exit of the annulus by 20%, 30%, 40%, 50% and 60% of the annular height. The results of the studies are summarized in Table 2. The same approach was employed for the case when the outer cylinder is subjected to rotation. It can be seen from Table 2 that the numerical simulations performed with extended domains 50% and 60% of annular height provide close results with experimental values for both cases viz: stationary and rotating outer cylinder. With this background, we have chosen 50% extended domain for further numerical studies. With 50% extended domain, a grid sensitivity study has been conducted to arrive at an optimum grid for numerical simulations. The summary of the results of grid sensitivity study is given in Table 3. The results are found to be insensitive to grid beyond the one with 1230098 cells, consisting of 594295 faces and 1392581 nodes. The final computational domain along with the grid used is shown in Fig. 3.

5 Results and discussions

5.1 Experimental results

The geometrical dimensions of the annulus considered in the present study are same as that of the experimental work to investigate natural convection in an annulus by Chouri et al. [36]. As part of a validation study, we performed natural convection experiments to compare the results with that reported by Chouri et al. [36]. The comparison of results illustrated in Fig. 4 shows good agreement. It may be noted that in Fig. 4 the temperature values corresponding to the non dimensional distance, z/H = 0 and 1 indicate the fluid temperature at the entry and exit of the annulus, respectively. Further, experiments were conducted to study the effect of rotation of the outer cylinder on the natural convection from the inner heated cylinder. In view of this, experimental runs were carried out with the different rotational speeds of the outer cylinder (10 to 460 rpm with incremental step of 10 rpm), possible with the present experimental set up. A better understanding of the heat transfer of the heated inner cylinder influenced by the rotation of the outer cylinder can be envisaged from the knowledge of local temperature distribution along the length of the heated cylinder, and for this purpose a plot showing the temperature, excess of the ambient, at different local positions on the heated cylinder for different rotational speeds (designated as dimensionless rotation parameter, ζ) of the outer cylinder was plotted and is depicted in Fig. 5. Higher temperature drop experienced by the inner cylinder than the natural convection case signifies the impact of the rotation of the outer cylinder on the energy transport mechanism.

In order to represent heat transfer characteristics, a dimensional analysis [37] was carried out to model the relation between the problem dependent and independent variables. The study concluded that Nusselt number is a function of rotational parameter ζ, radius ratio η and aspect ratio. The experiments were conducted for a wide range of rotational parameter $0 \leq \zeta \leq 526$, heat flux 80 W/m^2, 160 W/m^2 and 360 W/m^2 and radius ratio $\eta = 0.614$. The result of the experimental analysis shown in Figs. 6 and 7 indicates that heat transfer from the heated vertical inner cylinder is affected by the rotation of the outer cylinder. However, it is worth noting that the temperature of the heated cylinder was found to increase when the rotation parameter ζ is beyond 6. An important observation from Fig. 6 that three distinct regimes of heat transfer, namely, natural convection dominant, mixed convection and laminar forced convection dominant regimes are evident as the rotation parameter increases progressively

Table 2 Summary of domain independence study ($q'' = 80$ W/m^2, $\eta = 0.614$)

Rotational Reynolds number Reω	Measured surface temperature of the inner cylinder (K)	Numerically predicted surface temperature of heated inner cylinder (K) for different percentage of extended size of the domains(%)				
		20%.	30%.	40%.	50%.	60%
0	318.51	312.85	316.97	318.17	318.61	318.72
6760	313.81	308.10	311.41	313.51	314.01	314.08

Table 3 Summary of grid sensitivity study ($q'' = 80$ W/m^2, $\eta = 0.614$)

Rotational Reynolds number Reω	Number of cells	Measured surface temperatures (K) at different y−locations on the heated inner cylinder y in mm						Numerically predicted surface Temperature (K) at different y−locations on the heated inner cylinder y in mm					
		$y = 10$	$y = 95$	$y = 180$	$y = 265$	$y = 350$	$y = 435$	$y = 520$	$y = 605$	$y = 10$	$y = 95$	$y = 180$	$y = 265$	$y = 350$	$y = 435$	$y = 520$	$y = 605$
	125024									303.07	306.71	311.13	314.48	318.89	323.96	328.65	325.04
	238452									303.86	307.85	312.27	315.52	319.93	325.01	329.77	326.13
	486426									304.97	308.98	313.45	316.69	321.03	326.08	330.84	327.15
1156	**1023908**	**305.10**	**309.91**	**314.52**	**317.51**	**320.92**	**326.82**	**331.71**	**328.10**	**305.23**	**310.20**	**314.84**	**317.87**	**321.35**	**327.13**	**331.94**	**328.29**
	12300986									305.23	310.22	314.86	317.88	321.37	327.15	331.95	328.30

Highlighted data corresponds to comparison of experimentally measured and numerically predicted surface temperature for optimum grid

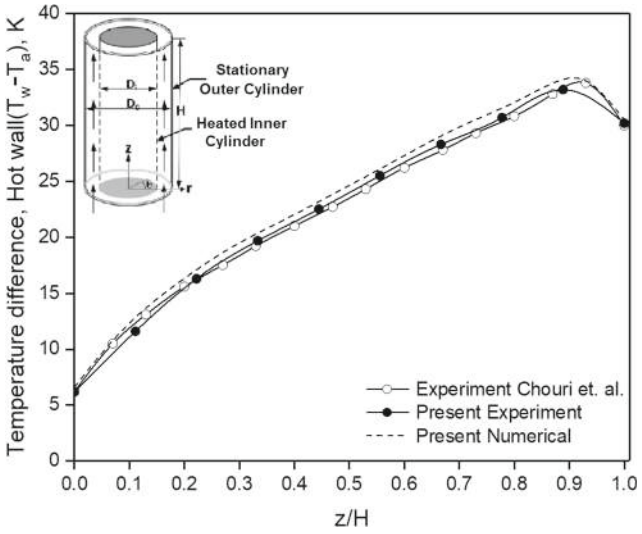

Fig. 4 Wall temperature distribution along the annular height of the heated inner cylinder ($q'' = 80$ W/m^2, $\eta = 0.614$)

until reaches a critical value, beyond which heat transfer performance deteriorates. A qualitative description of the heat transfer performance shown under the various regimes can be reasoned due to the changes in temperature and velocity fields happened owing to the change in the rotation parameter. The present experimental set up lacks facility to visualize the flow and thermal fields. Therefore, we carried out numerical analysis to solve the momentum and energy transport equations to visualize the flow and thermal fields.

5.2 Numerical results

Equations 7 to 11 have been solved numerically and the results are presented in terms of the dimensionless

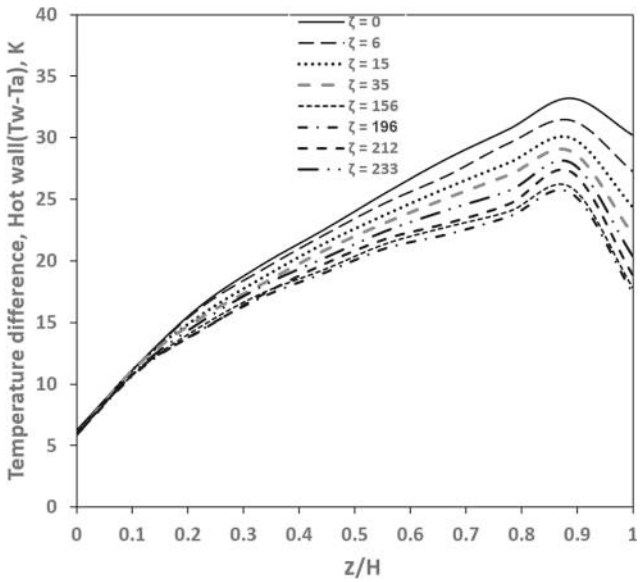

Fig. 5 Wall temperature measurements along the annular height of the heated inner cylinder for different ζ, ($q'' = 80$ W/m^2, $\eta = 0.614$)

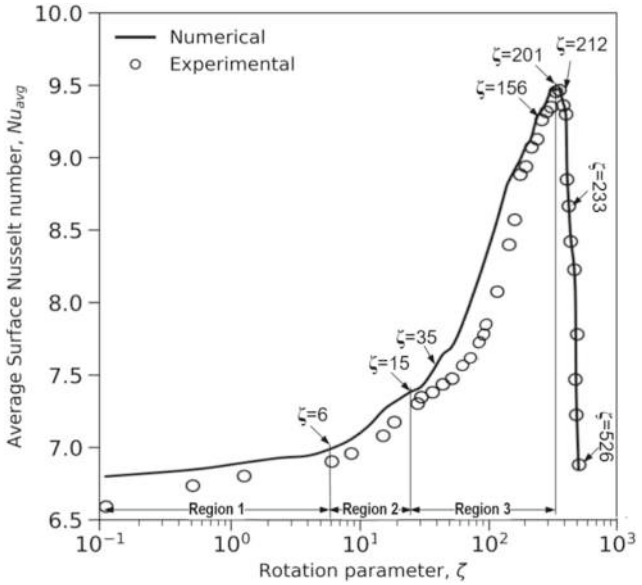

Fig. 6 Variation of Nusselt number with rotation parameter, ζ ($q'' = 80$ W/m^2, $\eta = 0.614$)

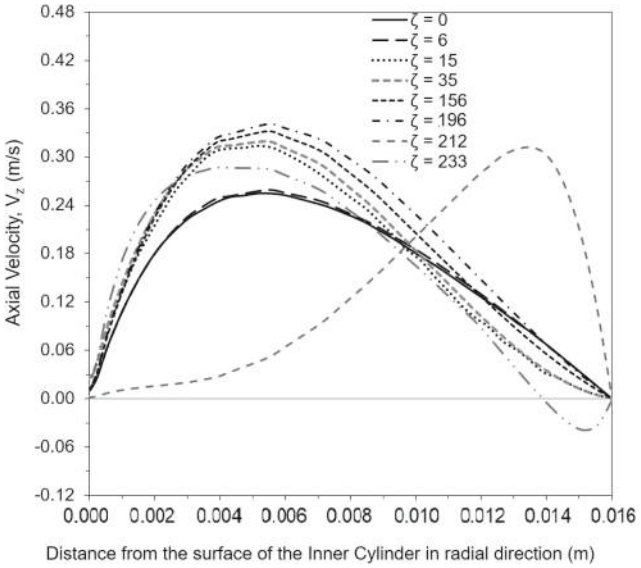

Fig. 8 Axial velocity across the annulus at the midheight of the annulus, ($q'' = 80$ W/m^2, $\eta = 0.614$)

parameters reported earlier. Firstly, numerical simulation of natural convection in stationary vertical cylindrical annulus was carried out and the results of simulations were compared with the experimental work of Chouri et al. [36]. Comparison of the results is shown in Fig. 4. The good agreement of results is indicative of appropriateness of the numerical model for describing the underlying physics. Further, numerical simulations were carried out with rotation imparted to the outer cylinder for the prediction of flow and thermal field that can provide valuable qualitative insight. Revisiting Fig. 6, shows agreement between numerically predicted average Nusselt number with experimental Nusselt number, as a function of rotational parameter. It can be observed from Fig. 6 that the increase in heat transfer rate is relatively constant up to rotational parameter $\zeta = 6$, above which it increases progressively with increasing rotation parameter. Interestingly, the slope of Nusselt number versus rotation parameter curve appears to change at rotation parameter $\zeta = 6$ and at $\zeta = 15$, and thereafter there is a steep increase in the Nusselt number up to rotation parameter $\zeta = 201$ was observed. Further increase in rotation parameter, beyond $\zeta = 201$, results in steep fall in Nusselt

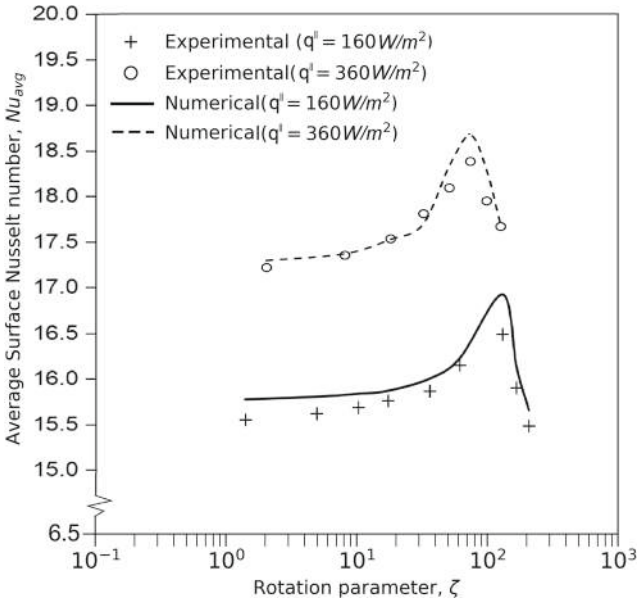

Fig. 7 Variation of Nusselt number with rotation parameter, ζ, for different heat flux, q''. ($\eta = 0.614$).

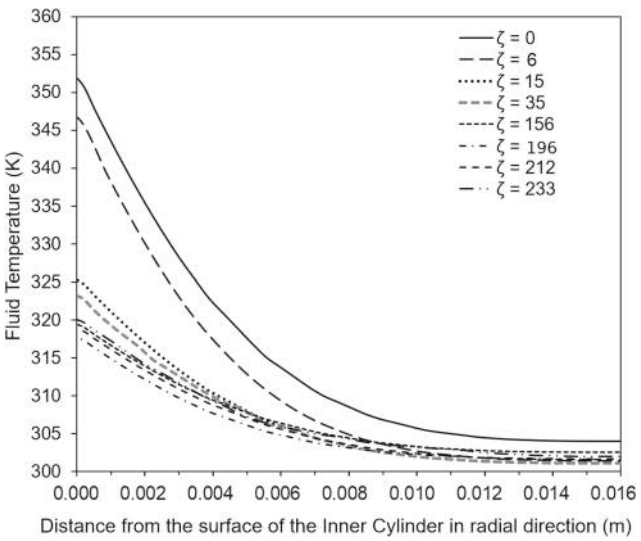

Fig. 9 Temperature distribution across the annulus at the midheight of the annulus, ($q'' = 80$ W/m^2, $\eta = 0.614$)

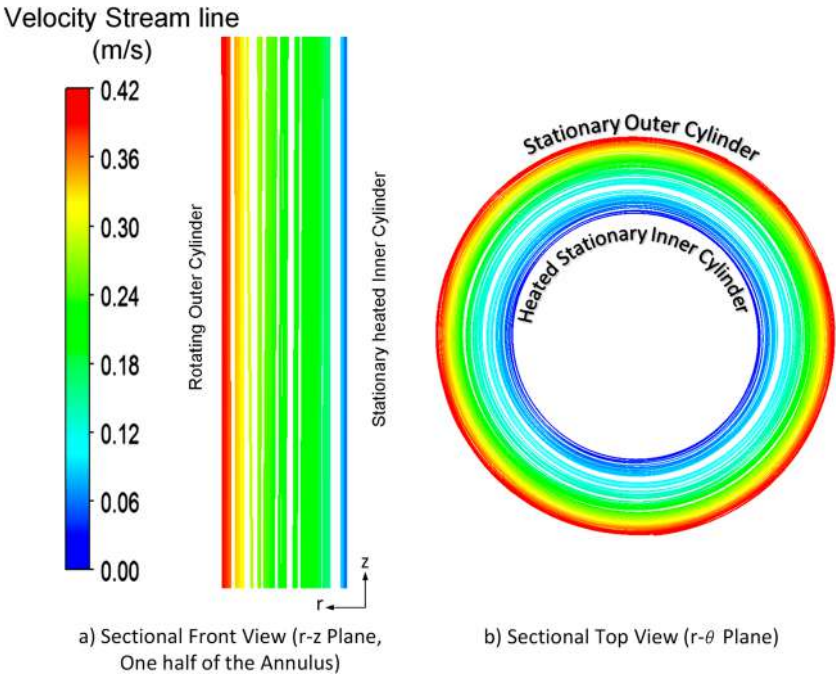

Fig. 10 Streamline pattern, ($\zeta = 6$, $q'' = 80$ W/m^2, $\eta = 0.614$)

number. The results reported here are mainly qualitative in nature but are not intended as an exact measure of the stability limit of the various regimes of flow. In order to explain the reason for variation in heat transfer rate, influenced by the rotation parameter, the plots of flow and and thermal field where drawn and are illustrated in Figs. 8, 9, 10, 11, 12, 13 and 14. The axial velocity profile and temperature profile drawn across annular gap at mid-height of the annulus are depicted in Figs. 8 and 9, respectively. Velocity and temperature profiles at $\zeta = 6$ follow similar trend as that of natural convection (ie $\zeta = 0$). Even though the velocity and temperature profile of the cases $\zeta = 0$ and $\zeta = 6$ follow same trend, a close examination reveals that velocity profile at $\zeta = 6$ appear slightly above velocity profile at $\zeta = 0$, consequently, fall in fluid temperature at $\zeta = 6$ was evident as shown in Fig. 9. The slight rise in the velocity profile at $\zeta = 6$ resulted in marginal increase of mass flow rate through the annulus as seen in Table 4. The result demonstrates that at low rotational speed the mean flow velocity distribution is weakly influenced by the rotation of the outer cylinder and fluid motion near the heated inner cylinder is aided mostly by buoyancy. It can, therefore, be inferred

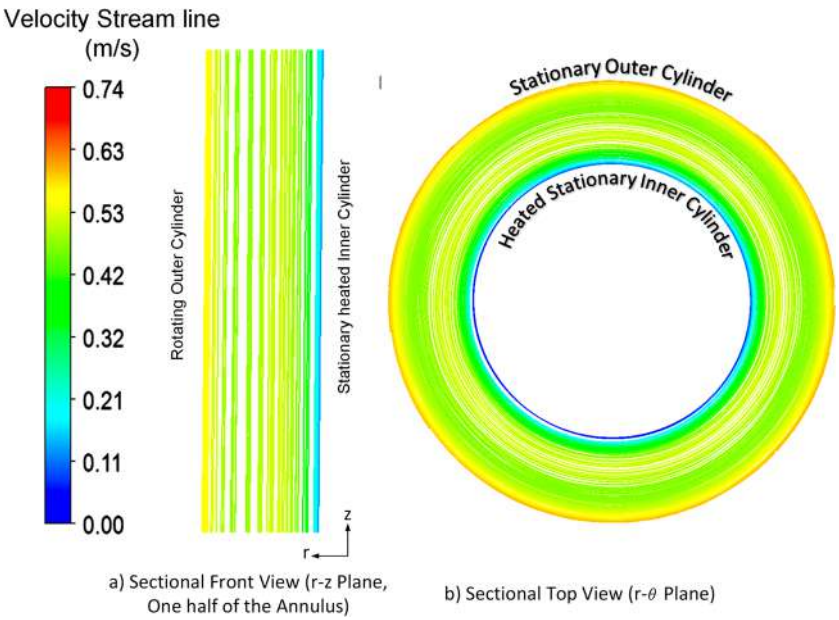

Fig. 11 Streamline pattern, ($\zeta = 15$, $q'' = 80$ W/m^2, $\eta = 0.614$)

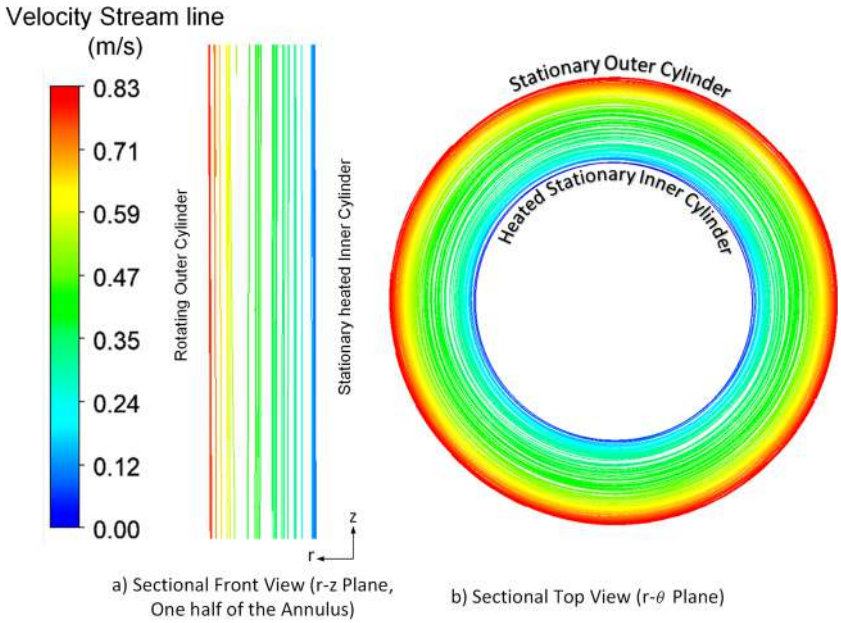

Fig. 12 Streamline pattern, ($\zeta = 35$, $q'' = 80$ W/m^2, $\eta = 0.614$)

that at low rotational speeds the mechanism of heat transfer is dominated by the buoyant force. As seen in Fig. 7, this regime of heat transfer can be identified as for $0 < \zeta \leq 6$. It is worth noting that the velocity boundary layer developed (see Fig. 8) at the outer wall signifies the wall confinement effect on convection in the annular gap and, therefore, the annular gap considered in this study comes under narrow gap annulus.

When the value of rotation parameter exceeds 6, a striking deviation in the trend of Nusselt number versus rotation parameter curve was observed (Fig. 6). This can be explained by noting that the greater centrifugal force exerted on the heavier fluid particles adjacent to the cold outer cylinder would have greater tendency to displace the lighter fluid particles adjacent to the hot inner cylinder. So, when the speed of rotation of the outer cylinder exceeds a critical value, the speed of rotation start influencing the natural convection. At moderate values of rotation parameter ($6 < \zeta \leq 15$) the centrifugal acceleration produced by rotational effect assist the buoyancy driven flow caused by axial temperature gradient. The non linear dependency of Nusselt number with rotation parameter, in the range $6 < \zeta \leq$

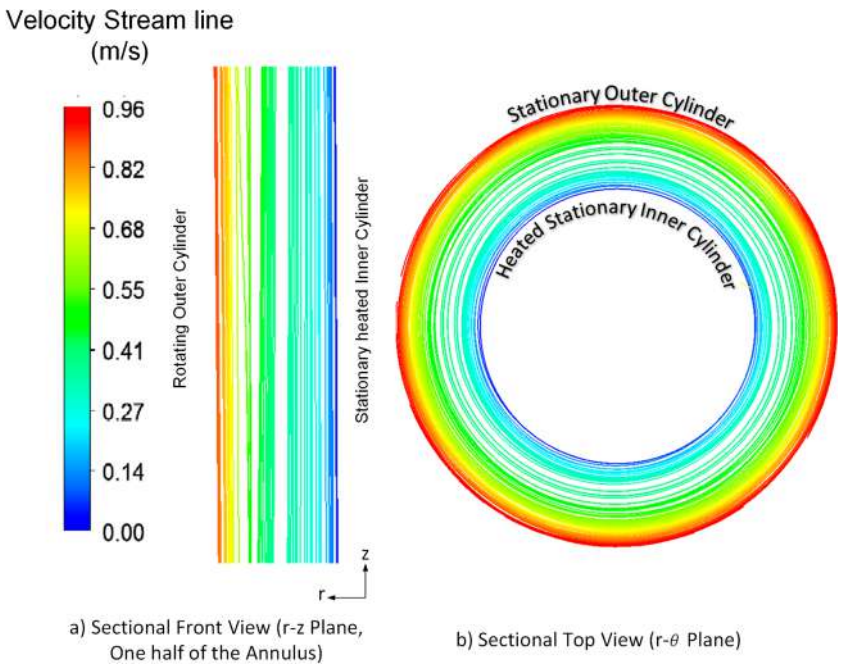

Fig. 13 Streamline pattern, ($\zeta = 156$, $q'' = 80$ W/m^2, $\eta = 0.614$)

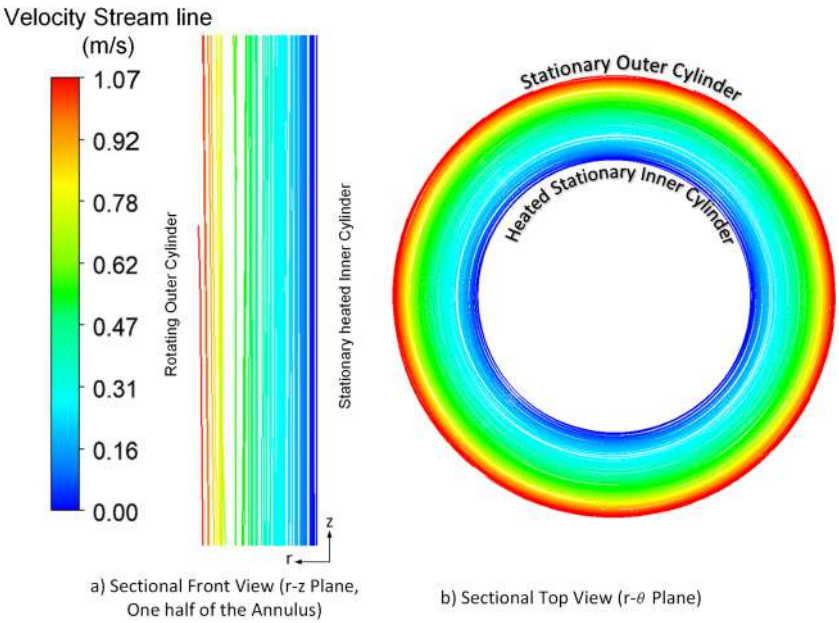

Fig. 14 Streamline pattern, ($\zeta = 196$, $q'' = 80$ W/m^2, $\eta = 0.614$)

15, reveals the fact that the centrifugal and buoyant forces complimenting each other in prompting the transport of heat energy. It is therefore, reasoned that mixed convection regimes exist in the aforesaid range of rotation parameter. Clearly in this range of rotation parameter, the flow structure and thermal fields are determined by the interaction of gravitational and centrifugal fields. The axial velocity profile shown in Fig. 8 together with the streamline contours depicted in Figs. 10 and 11 demonstrate that the forced flow induced by the centrifugal effect augments upward flow of fluid along the vicinity of the heated inner cylinder. Consequently mass flow rate through the annulus was found to increase compared to the case of buoyant convection as can be seen in Table 4.

As the speed of rotation of the outer cylinder increases, the centrifugal effect becomes more significant and, therefore, the action of buoyant force is getting reduced. However, it is imperative that the action of buoyant force persist in determining the flow structure until the speed of rotation exceed a threshold value. As long as the action of buoyant force continue to act, the higher centrifugal forces together with buoyant force causes an increase in mean velocity in the annular gap, with the velocity peak shifting towards the outer rotating cylinder as seen in Fig. 8. The centrifugal force was not high enough to alter the flow field significantly therefore, the main flow appears axial. This is also evident from the streamline contours plots in Figs. 11, 12, 13 and 14 for the cases $\zeta = 15$, $\zeta = 35$, $\zeta = 156$ and $\zeta = 196$. The stronger induced flow originated by larger centrifugal effects produced by the rotation of the outer cylinder supplements the mass flow rate through the annulus, consequently, mass flow rate increases as compared to that caused by low rotational speeds (Table 4). The fluid mass entrainment caused by the forced rotation of the outer cylinder can be regarded as fluid flow driven by an external source in the case of a typical forced convection problem. So the heat transfer can be regarded as forced convection due to the rotation of outer cylinder. As mentioned earlier the numbers shown here are not the exact measure of the demarcation of heat transfer regimes, but are largely qualitative in describing the nature of flow structure experienced under various regimes of heat transfer. The physics of transport mechanisms under this regime of heat transfer remains unchanged until the effect of buoyant forces become unimportant consequently, the heat transfer rate increases fairly in a steady manner with increase in rotation parameter, as seen in Fig. 6. But when the speed of rotation of the outer cylinder has reached to a point at which secondary flow consisting of vortices begins to appear in the vicinity of the outer cylinder, the heat transfer

Table 4 Mass flow rate through the annulus ($q'' = 80$ W/m^2, $\eta = 0.614$, AR = 38.75)

Mass flow rate kg/min	Rotation parameter ζ								
	0	6	15	35	156	196	201	212	233
$\dot{m}$	0.039	0.040	0.044	0.046	0.049	0.050	0.051	0.050	0.037

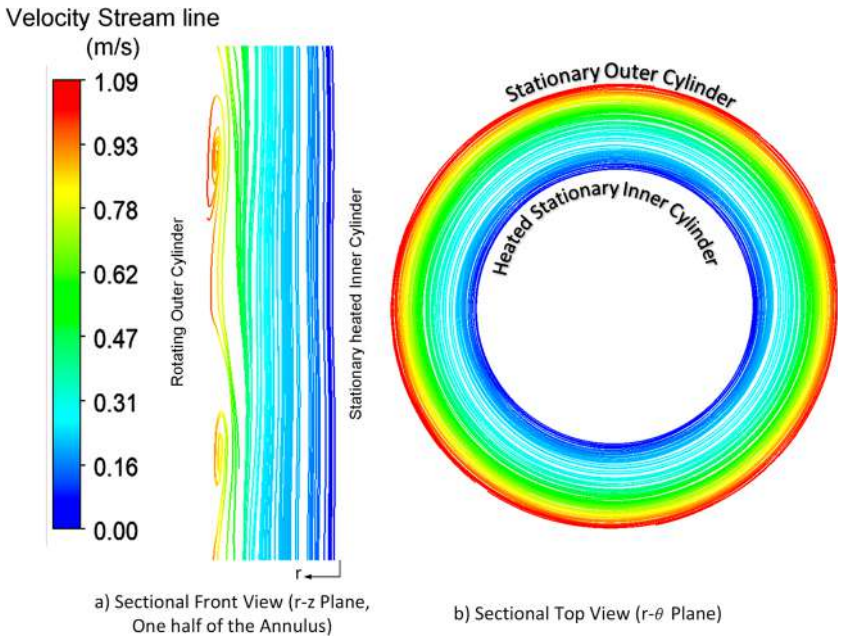

Fig. 15 Streamline pattern, ($\zeta = 201$, $q'' = 80$ W/m^2, $\eta = 0.614$)

performance of the inner cylinder starts to deteriorate. This happens when the speed of rotation is significantly high such that the centrifugal force exceeds that of gravity. For the present case, the onset of vortices near the rotating outer cylinder was noticed at around $\zeta = 201$. Thereafter, a sharp decay in heat transfer from the inner cylinder was observed. Because of the steadily increasing nature of heat transfer rate with increase in rotation parameter, ζ observed during the range $6 < \zeta \leq 201$, the convection corresponding to aforementioned range of rotation parameter is considered to be forced convection dominant regime.

With further increase in rotation parameter beyond 201, the buoyant convection is suppressed by stronger centrifugal effects and centrifugal effects become the driving factor in determining the flow structure. With stronger rotation, the centrifugal effects become more important in the vicinity of the outer cylinder, causing the fluid to move towards the outer cylinder. Consequently, the bulk flow is displaced towards the outer cylinder with vortices developed around the outer cylinder. This forced flow resulting from the strong centrifugal effect tends to stratify the flow field in the radial direction. The mal-distribution of the flow field leads to fall

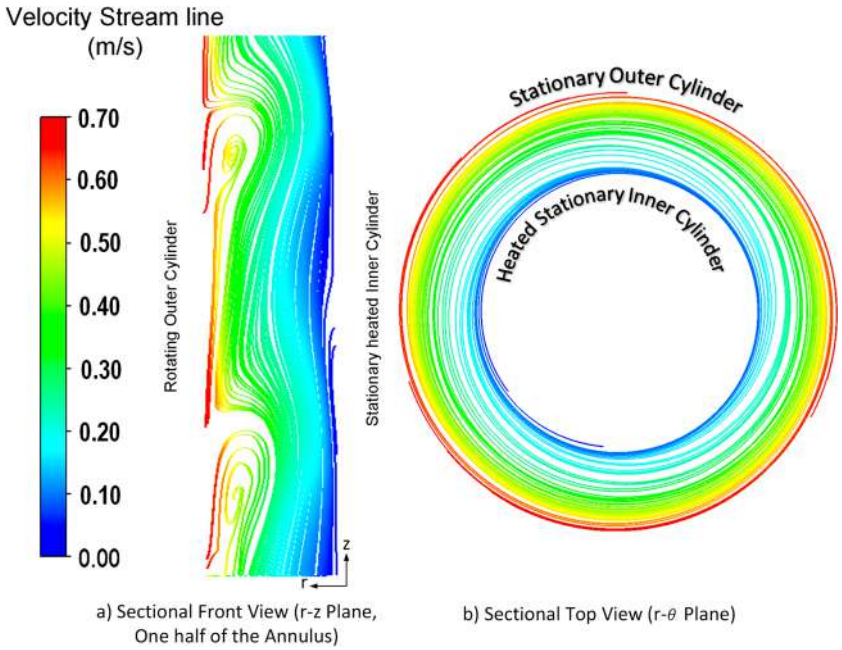

Fig. 16 Streamline pattern, ($\zeta = 212$, $q'' = 80$ W/m^2, $\eta = 0.614$)

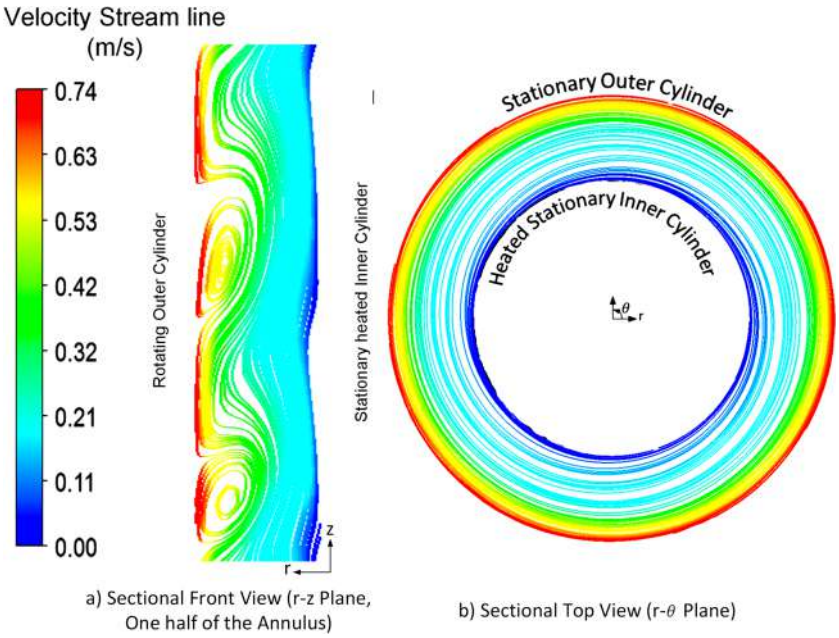

Fig. 17 Streamline pattern, ($\zeta = 233$, $q'' = 80$ W/m^2, $\eta = 0.614$)

in mass flow rate through the annulus as can be seen in Table 4. It is therefore inferred that the mean flow velocity distributions are clearly affected by the rotation of the outer cylinder when the rotation parameter exceeds a value around 201. The axial velocity profile and stream function contours depicted in Figs. 6, 15, 16 and 17 respectively demonstrate the aforesaid characteristics features of the flow. As expected, the temperature field is also affected by amendment of flow structure caused by the presence of vortices in the vicinity of the outer cylinder. Figure 18 illustrates the modification of temperature field envisaged as a result of change in rotation parameter. Add to this the strength of vortices in the vicinity of the outer cylinder goes on increasing with increase in rotation parameter (Figs. 15, 16 and 17). The stratification of flow field caused by the change in the flow pattern has resulted in significant reduction in mean heat transfer, ones the rotation parameter exceeds a value around 201. So, as can be seen in Fig. 6,

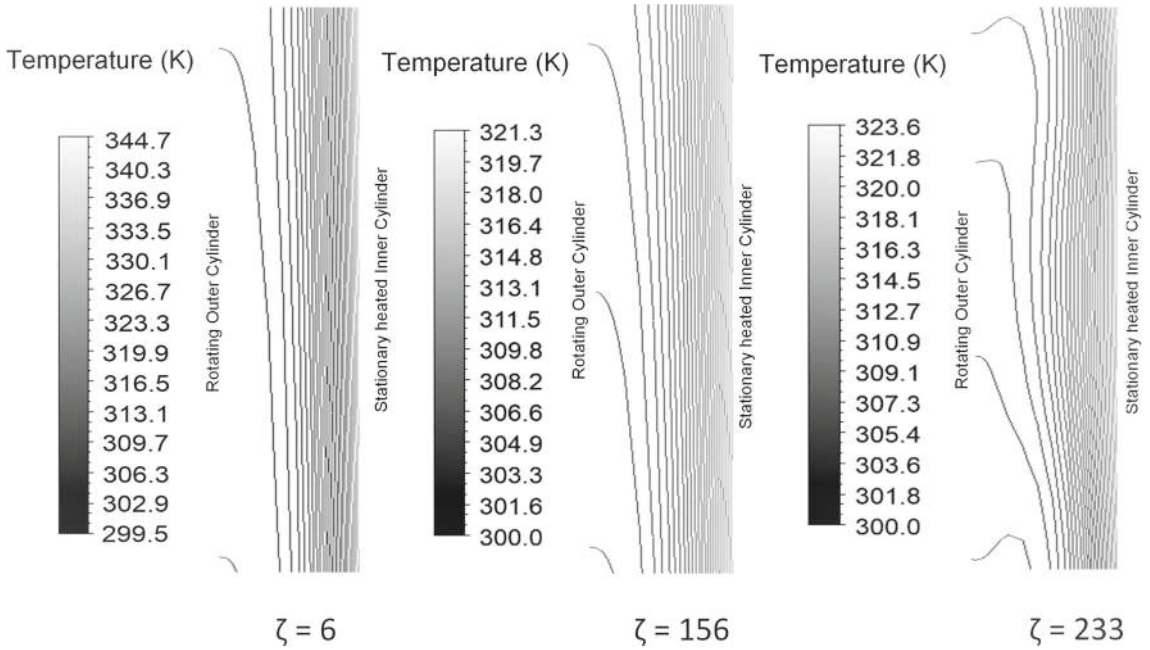

Fig. 18 isotherms for different ζ, ($q'' = 80$ W/m^2, $\eta = 0.614$)

a sharp drop in mean Nusselt number at the wall of the inner cylinder was observed when the speed of rotation has exceeded a limiting value around 201.

6 Conclusions

Experimental and numerical studies were conducted to understand convective heat transfer in a vertical annular gap formed between a heated stationary inner cylinder and a rotating cold outer cylinder. The impact of rotation of outer cylinder on heat convection from the inner cylinder was analyzed and discussed. The important results of the study are summarized below

- The results of our natural convection experiments agree well with that of the experimental work reported by Chouri et al. [36].
- The heat transfer rate from the stationary heated inner cylinder was found to increase progressively with increase in speed of rotation of the cold outer cylinder until the speed of rotation of the outer cylinder exceeds a critical value.
- Three laminar heat convection regimes namely natural convection dominant, mixed convection and forced convection dominant regimes were identified in the increasing phase of heat transfer with speed of rotation.
- Significant reduction in heat transfer rate from the heated inner cylinder was observed when the speed of rotation of the outer cylinder exceeds the limiting value
- The physics of flow and energy transport mechanism associated with various regimes of heat transfer was explored and discussed
- The numerically simulated flow and thermal fields have provided valuable information to substantiate experimental data

Appendix

Details of Uncertainity analysis

$$Q = VI, h = \frac{Q}{A\nabla T}, Nu = \frac{hd}{k}$$

$$\sigma_Q = \sqrt{\left[\frac{\partial Q}{\partial V}\sigma_V\right]^2 + \left[\frac{\partial Q}{\partial I}\sigma_I\right]^2} \bullet$$

$$\sigma_h = \sqrt{\left[\frac{\partial h}{\partial Q}\sigma_Q\right]^2 + \left[\frac{\partial h}{\partial A}\sigma_A\right]^2 + \left[\frac{\partial h}{\partial \nabla T}\sigma_{\nabla T}\right]^2} \bullet$$

$$\sigma_{Nu} = \sqrt{\left[\frac{\partial Nu}{\partial h}\sigma_h\right]^2 + \left[\frac{\partial Nu}{\partial d}\sigma_d\right]^2} \bullet$$

References

1. Kuehn TH, Goldstein RJ (1976) An experimental and theoretical study of natural convection in the annulus between horizontal concentric cylinders. J Fluid Mech 74:695–719
2. Kuehn TH, Goldstein RJ (1978) An experimental study of natural convection heat transfer in concentric and eccentric horizontal cylindrical annuli. ASME J Heat Transf 100:635–640
3. Alawadhi EM (2008) Natural convection flow in a horizontal annulus with an oscillating inner cylinder using Lagrangian–Eulerian kinematics. Comput Fluids 37:1253–1261
4. Fenot MA (2011) review of heat transfer between concentric rotating cylinders with or without axial flow. Int J Thermal Sci 50:1138–1155
5. Rahimi AB, Abedini Ahad (2013) Numerical study of three-dimensional mixed convection in an eccentric annulus. J Thermophys Heat Transf 27:719–732
6. Sefid M, Izadpanah E (2013) Developing and fully developed non-Newtonian fluid flow and heat transfer through concentric annuli. J Heat Transf 135:071701–708
7. Yang CS, Jeng DZ, Tang UH, Gau C (2009) Flow and heat transfer of natural convection in horizontal annulus with a heating element on inner cylinder. J Heat Transf 131:082502-1–082502-6
8. Tachibana F, Fukui S, Mitsumura H (1960) Heat transfer in an annulus with an inner rotating cylinder. Bull JSME 3:119–123
9. Kuzay TM, Scott CJ (1977) Turbulent heat transfer studies in annulus with inner cylinder rotation. J Heat Transf 99:12–19
10. Sarhan A, El-Shaarawi MAI (1981) Developing laminar free confection in an open ended vertical annulus with a rotating inner cylinder. Trans ASME 103:552–558
11. El-Shaarawi MAI, Sarhan A (1982) Combined forced-free laminar convection in the entry region of a vertical annulus with a rotating inner cylinder. Int J Heat Mass Transf 25:175–186
12. Fusegi T, Farouk B, Ball KS (1986) Mixed-convection flows within a horizontal concentric annulus with a heated rotating inner cylinder. Numers Heat Transf Part A: Appl 9:591–604
13. Hessami MA, Devahl Devis G, Leonardi E, Reizes JA (1987) Mixed convection in vertical, cylindrical annuli. Int J Heat Mass Transf 30:151–164
14. Ball KS, Farouk B (1987) On the development of Taylor vortices in a vertical annulus with a heated rotating inner cylinder. Int J Numer Methods Fluids 7:857–867
15. Ball KS, Farouk B, Dixit VC (1989) An experimental study of heat transfer in a vertical annulus with a rotating inner cylinder. Int J Heat Mass Transf 32:1517–1527
16. Lueptow RM, Docter A, Min K (1992) Stability of axial flow in an annulus with a rotating inner cylinder. Phys Fluids A: Fluid Dyn 4(11):2446–2455
17. Rothe T, Pfitzer H (1997) The influence of rotation on turbulent flow and heat transfer in an annulus between independently rotating tubes. Heat Mass Transf 32:353–364
18. Char M-I, Hsu Y-H (1998) Numerical prediction of turbulent mixed convection in a concentric horizontal rotating annulus with low-Re two-equation models. Int J Heat Mass Transf 41:1633–1643
19. Yoo J-S (1998) Mixed convection of air between two horizontal concentric cylinders with a cooled rotating outer cylinder. Int J Heat Mass Transf 41:293–302
20. Lee TS (1998) Numerical study of mixed heat and fluid flow in annuli of heated rotating cylinders. Int J Comput Fluid Dyn 9:151–163
21. Habib MA, Negm AAA (2001) Laminar mixed convection in horizontal concentric annuli with non-uniform circumferential heating. Heat Mass Transf 37:427–435

22. Venkatachalappa M, Sankar M, Natarajan AA (2001) Natural convection in an annulus between two rotating vertical cylinders. Acta Mech 32:173–196
23. Lee JS, Xu X, Pletcher RH (2005) Effects of wall rotation on heat transfer to annular turbulent flow: outer wall rotating. J Heat Transf 127(8):830–838
24. Howey DA, Childs PRN, Holmes AS (2012) Air-gap convection in rotating electrical machines. IEEE Trans Ind Electron 59:1367–1375
25. Dyko MP, Vafai K (2001) Three-dimensional natural convective states in a narrow-gap horizontal annulus. J Fluid Mech 445:1–36
26. Venkateshan SP (2015) Mechanical measurements-Page No 346-349, 2nd edn. Ane Books Pvt. Ltd, India
27. Kline SJ, Mcclintock FA (1953) Describing uncertainties in single sample experiments. Mech Eng 75:3–8
28. Kline SJ (1985) The purposes of uncertainty analysis. J Fluids Eng 107:153–160
29. (2006) ANSYS, Incor., 275, Technology Drive, Canonsburg
30. Hypermesh 13, Altair, Troy, Michigan, USA
31. Drikakis D, Rider W (2005) High-resolution methods for incompressible and low-speed flows, 1st edn. Springer, New York
32. Bazdidi-Tehrani F, Moghaddam S, Aghaamini M (2018) On the validity of Boussinesq approximation in variable property turbulent mixed convection channel flows. Heat Transf Eng 39(5):473–491
33. da Silva AK, Lorente S, Bejan A (2004) Optimal distribution of discrete heat sources on a wall with natural convection. Int J Heat Mass Transf 47:203–214
34. Manca O, Nardini S, Ricci D, Tamburrino S (2011) Numerical study of transient natural convection in air in vertical divergent channels. Numer Heat Transf, Part A: Appl 60(7):580–603
35. Rajkumar MR, Venugopal G, Anil Lal S (2011) Natural convection with surface radiation from a planar heat generating element mounted freely in vertical channel. Heat Mass Transf 47:789–805
36. Choueiri GH, Tavoularis S (2011) An experimental study of natural convection in vertical, open-ended, concentric, and eccentric annular channels. ASME J Heat Transf 133:37. 122503-9
37. Gibblings JC (2011) Dimensional analysis. Springer, New York

Affiliations

V. K. Chithrakumar[1] · G. Venugopal[2] · M. R. Rajkumar[1]

V. K. Chithrakumar
chithrakumarvk@gmail.com

G. Venugopal
gvenucet@gmail.com

[1] Advanced Thermo Fluid Research Lab, Department of Mechanical Engineering, College of Engineering Trivandrum, Trivandrum, India

[2] Department of Mechanical Engineering, Goverment Engineering College, Thrissur 680009, India